

On the mechanism of acceleration behavior of plasma bullet

S. Wu, X. Lu, and Y. Pan

Citation: *Physics of Plasmas* (1994-present) **21**, 073509 (2014); doi: 10.1063/1.4890490

View online: <http://dx.doi.org/10.1063/1.4890490>

View Table of Contents: <http://scitation.aip.org/content/aip/journal/pop/21/7?ver=pdfcov>

Published by the [AIP Publishing](#)

Articles you may be interested in

[The production mechanisms of OH radicals in a pulsed direct current plasma jet](#)

Phys. Plasmas **21**, 093513 (2014); 10.1063/1.4895496

[Multiple \(eight\) plasma bullets in helium atmospheric pressure plasma jet and the role of nitrogen](#)

Appl. Phys. Lett. **103**, 224105 (2013); 10.1063/1.4833638

[Ion acceleration by laser hole-boring into plasmas](#)


AIP Conf. Proc. **1507**, 814 (2012); 10.1063/1.4773803


[Electrical potential measurement in plasma columns of atmospheric plasma jets](#)

J. Appl. Phys. **112**, 103305 (2012); 10.1063/1.4766756


[Forcing mechanisms of dielectric barrier discharge plasma actuators at carrier frequency of 625 Hz](#)

J. Appl. Phys. **110**, 113301 (2011); 10.1063/1.3664695

A collection of five pieces of industrial vacuum equipment from Pfeiffer Vacuum. From top-left to bottom-right: a red rectangular turbopump, a cylindrical stainless steel backing pump, a white rectangular turbopump, a red cylindrical turbopump with a long metal shaft, and a large, complex stainless steel chamber or component.

 Vacuum Solutions from a Single Source

- Turbopumps
- Backing pumps
- Leak detectors
- Measurement and analysis equipment
- Chambers and components

PFEIFFER  **VACUUM**

On the mechanism of acceleration behavior of plasma bullet

S. Wu, X. Lu,^{a)} and Y. Pan

State Key Laboratory of Advanced Electromagnetic Engineering and Technology, Huazhong University of Science and Technology, Wuhan, Hubei 430074, China

(Received 10 May 2014; accepted 7 July 2014; published online 18 July 2014)

Two special experiments are designed to study the mechanism of the acceleration behavior of a plasma bullet when it exits a nozzle. First, a T-shape device is used to simulate the air diffusion when a plasma plume exits the nozzle. It is found that adding just 1% of N₂, O₂, or air to the main working gas He results in the acceleration of the plasma bullet. Second, materials of different permittivity are added to the left part of the outside of the tube. The experimental results show that the plasma bullet accelerates at the moment when it enters into the right part of the tube where there is no extra material on the outside of the tube. These two experiments confirm that the acceleration behavior of the plasma bullet when it exits the nozzle is due to the air diffusion, hence Penning ionization, and the permittivity change when the bullet exits the nozzle, for example, from a tube with high permittivity to air with low permittivity. Besides, electric field measurements show that the electric field in the bullet head increases when the plasma bullet accelerates. This confirms the electric field driven nature of the plasma bullet propagation. © 2014 AIP Publishing LLC.
[\[http://dx.doi.org/10.1063/1.4890490\]](http://dx.doi.org/10.1063/1.4890490)

I. INTRODUCTION

Room temperature atmospheric-pressure plasma jets (RT-APPJs) have recently attracted growing interest, motivated by their potential applications such as materials processing^{1,2} and plasma medicine.^{3–9} Plasma jets usually generate plasmas in a dielectric tube (diameter in mm range) first, then the plasmas expand into ambient air due to the flow of noble gas such as He or Ar. The length of the plasma plume in ambient air could reach 10 cm or longer.¹⁰ RT-APPJs generate plasmas in open space, thus there is no limitation on the size of objects to be treated while short-life-time reactive species including charge particles can reach the objects to be treated, which is very attractive for applications such as plasma medicine.

Several research groups demonstrated that these plasma jets are not continuous jets but discrete bullet-like plasma volumes travelling at speeds of 10⁴–10⁵ m/s.^{11–15} According to experimental and modeling studies,^{16–22} it is now commonly accepted that the “plasma bullets” are ionization waves, which are quite similar to cathode-directed streamers.

Both high-speed photography and time-resolved optical emission spectroscopy studies reveal that, when the plasma bullets propagate out of a dielectric tube nozzle, the bullet velocities increase first and reach a maximum value, then they decrease slowly during the further propagation phase.^{12,23–25} However, the mechanisms of the acceleration behavior of the plasma bullets are not yet well understood. On one hand, Wu *et al.* in 2011²⁶ reported that, when both the working gas and the surrounding gas are He/N₂ mixture, the velocity of the plasma bullet increases as soon as it propagates out of the nozzle into a chamber. On the other hand, when both the working gas and the surrounding gas are He, the velocity of the plasma bullet decreases when it propagates into the chamber. It was

concluded that the Penning reaction between the He metastable states and N₂ molecules plays an important role in the acceleration of the plasma bullet when it propagates out of the nozzle. Furthermore, numerical results show that the peak velocity of the plasma bullet increases from 2.08 × 10⁵ m/s to 2.65 × 10⁵ m/s when the air impurity level varies from 10 ppm to 10 000 ppm.²⁷ It was concluded that the additional N₂ in the air stimulates the Penning ionization, which facilitates the volume ionization and hence, accelerates the propagation of the plasma bullet. However, by turning the Penning reactions on and off in their models, Naidis¹⁷ and Breden *et al.*¹⁸ have shown that the Penning ionization is not essential for the plasma bullets propagation. Besides, Mericam-Bourdet *et al.*²⁴ proposed that the plasma bullet is formed by a surface wave propagating at the interface between two media, and the propagation velocity depends on the dielectric constant of the two adjacent media. The higher the dielectric constant of the outer layer, the lower is the speed. This is believed to be the reason why the speed of the plasma bullet increases when it exits the nozzle. Furthermore, Jansky and Bourdon²⁸ simulated the dynamics of the plasma plume inside and outside of the tube to study the influence of the change of permittivity of the medium surrounding the plasma plume. They found out that the propagation speed of the plasma bullet increases as it exits from the glass tube with a dielectric constant of four into the surrounding tube with a dielectric constant of one.

According to the above discussion, there are two main possible reasons for the acceleration of the plasma bullets when they exit from the tube into the surrounding air. One reason is due to the diffusion of N₂ from the air, which results in the Penning ionization and finally leads to the acceleration of the plasma bullets. Another one is due to the change of the permittivity of the medium surrounding the plasma plume. Because all the tubes used for the plasma plume production have permittivity higher than that of air. When the plasma plumes exit from the tube into the

^{a)} Author to whom correspondence should be addressed. Electronic mail: luxinpei@hotmail.com

surrounding air, the permittivity of the medium surrounding the plasma plumes decreases, which results in the acceleration of the plasma bullets. This is similar with the surface discharge.

Up to now, it is still not known whether both of the two possible reasons play a role in the acceleration of the plasma bullets when they exit the nozzle. To clearly understand the acceleration mechanism of the plasma bullets when they exit from a dielectric tube, it is worth investigating the effect of N_2 diffusion and the change of the permittivity of the medium surrounding the plasma plumes separately. In this work, two dedicated experiments are designed to investigate the acceleration mechanism of the plasma bullets when they exit the nozzle. First, a T shape tube is used in the experiment. The vertical part of the T tube is used to simulate the effects of the air diffusion. It is found that, when 1% of N_2 , O_2 , or air is added from the vertical tube to the He gas flow in the horizontal tube, the lengths of the plasma plumes for all three cases increase slightly. Besides, the propagation velocities of the plasma bullets for the three cases all increase significantly when the bullets propagate through the junction point of the T tube.

Second, an additional tube is placed on the left side part of the outside of the tube to simulate the change of the permittivity. It is found that the change of the permittivity surrounding the plasma plumes also affects the propagation velocity of the plasma bullet.

This paper is organized as follows. The experimental setup is described in Sec. II. The experimental results are presented in Sec. III. Finally, the discussion of the experimental results and a brief conclusion of this work are presented in Sec. IV.

II. EXPERIMENTAL SETUP

The discharge device consists of a plasma jet generated in a T shape tube with He flowing horizontally and N_2/O_2 /air flowing vertically, as shown in Fig. 1. The device is driven by a pulsed dc generator (voltage amplitudes up to 10 kV, repetition rate up to 10 kHz, pulse width variable from 200 ns to dc). The high-voltage (HV) electrode is made of a stainless steel needle, which is connected to the pulse generator. The HV electrode is placed inside the horizontal tube with a distance of 3.5 cm away from the cross point A. The radius of the needle tip is about 100 μm . The inner diameters of the horizontal and vertical tubes are 2 mm and 1 mm, respectively. To keep the ambient air contamination from the right end of the tube as low as possible, another tube with a length of 3 m is connected to the right end of the quartz tube. When the He gas flow rate is 1 l/min, the amount of air

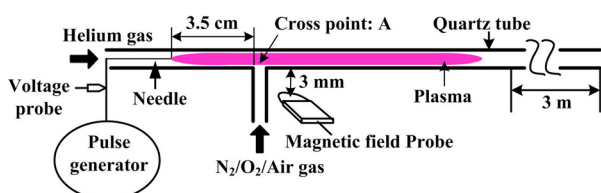


FIG. 1. The schematic of the experimental setup.

around the plasma plume is even lower than the amount of impurities in research-grade He, which is confirmed by the simulation results by using FLUENT software.²⁹

A P6015 Tektronix voltage probe and a magnetic field probe (AZ-530-M, frequency bandwidth from 0.1 MHz to 1 GHz) are used to measure the high voltage and the magnetic field signal radiated from the plasma plume, respectively. The magnetic field probe is mounted 3 mm below the plasma plume close to the cross point A, as shown in Fig. 1. The magnetic field probe is based on small area wire loops with few turns. It is worth pointing out that the measured magnetic field signal is proportional to the discharge current of the plasma plume. Detailed descriptions of the magnetic probe can be found in Ref. 30. The measured signals are recorded by a Tektronix DPO7104 wideband digital oscilloscope. A fast intensified charge-coupled device (ICCD) camera (Princeton Instruments, Model: PIMAX2, exposure time down to 0.5 ns, jitter time down to 1 ns) is used to capture the dynamics of the discharge.

III. EXPERIMENTAL RESULTS

A. Photos of the discharge

When the high voltage is applied to the needle, and He gas is injected into the horizontal tube with flow rate of 1 l/min, a plasma plume is generated inside the horizontal tube, as shown in Fig. 2(a). When 1% N_2 , O_2 , or air is added from the vertical tube, the lengths of the plasma plumes all become slightly longer than the case of He only.

B. Voltage-magnetic field signal waveforms

To measure the voltage on the needle and the magnetic field signal emitted from the plasma plume, a P6015 Tektronix high-voltage probe and a magnetic field probe (AZ-530-M) are used. Figure 3 shows the waveforms of the applied voltage and magnetic field signal emitted from the plasma plumes *versus* time. The peak values of the magnetic field signals are about 8.4 dbm, 7.7 dbm, 6.5 dbm, and 5.7 dbm for 1% N_2 , 1% air, 1% O_2 , and pure He, respectively. Because the magnetic field signal is proportional to the discharge current as reported

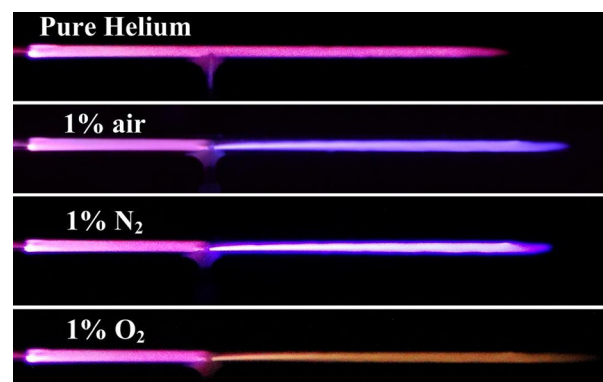


FIG. 2. The photographs of the plasma plumes for He only and He with 1% air, N_2 , or O_2 added from the vertical tube. (a) He. (b) He/air (1%). (c) He/ N_2 (1%). (d) He/ O_2 (1%). The total gas flow rates are all fixed at 1 l/min. The electric pulse parameters: pulse voltage of 7 kV, pulse frequency of 5 kHz, and pulse width of 800 ns.

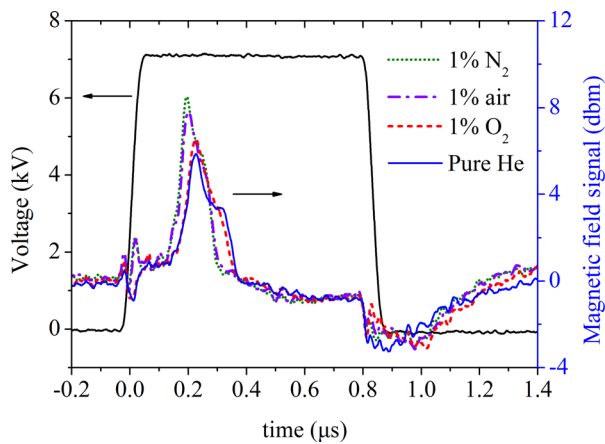


FIG. 3. The voltage and magnetic field signal waveforms *versus* time for different added gases. The discharge parameters are the same as in Fig. 2.

in Ref. 30, it can thus be concluded that the discharge current increases when 1% of N_2/O_2 /air gases is added.

C. Dynamics of the discharge

As pointed out in the Introduction, the small amount of the added gas (1% of N_2 , O_2 , or air) flowing from the vertical tube into the horizontal tube is used to simulate the diffusion of the surrounding gas into the He gas stream. Under such conditions, the permittivity of the medium surrounding the plasma plumes is constant along the whole tube. In this way, one can clarify the role of the diffusion of the surrounding gas on the acceleration of the plasma bullets when they exit the nozzle.

In the following, the dynamics of the plasma plumes with or without added gases are captured by an ICCD camera. Figures 4 and 5 show the dynamics of the plasma plumes for He only and He with 1% added air, respectively. In the case of He only as shown in Fig. 4, the propagation velocity and the shape of the plasma bullet have no obvious change before and after the cross point A. However, when 1% of air is added from the vertical tube, as soon as the plasma bullet

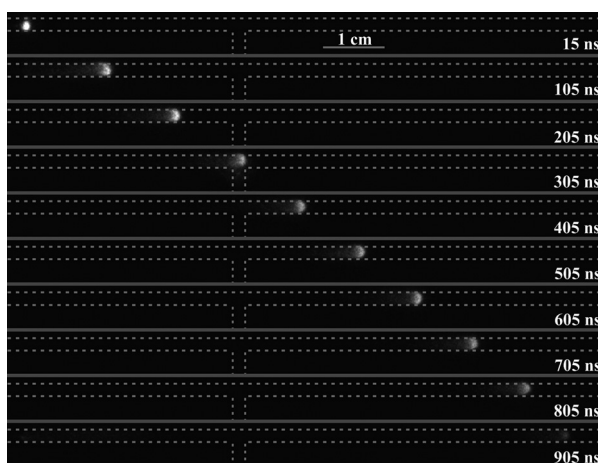


FIG. 4. High-speed images of the plasma for pure He with flow rate of 1 l/min. The exposure time is fixed at 5 ns. Each image is an integrated picture of 50 shots at the same delay time. The time labels at the right side of each image correspond to the times in Fig. 3. The electric pulse parameters are the same as in Fig. 2.

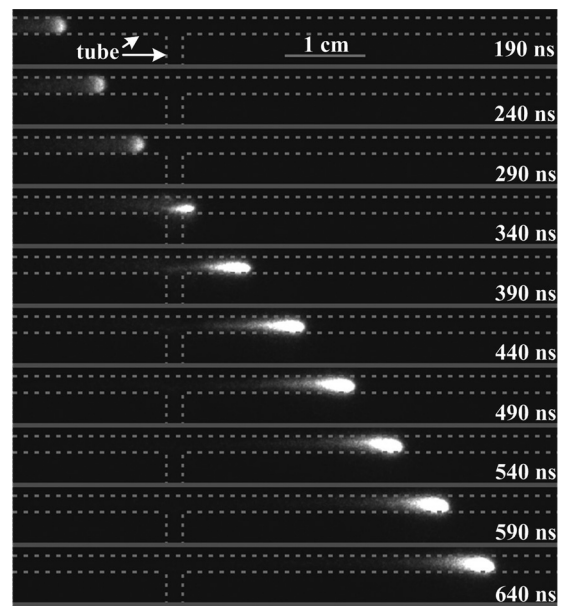


FIG. 5. High-speed images of the discharge for the case of 1% air added from the vertical tube. The total gas flow rate is fixed at 1 l/min. All other parameters are the same as in Fig. 4.

pass through the junction point, its optical emission intensity increases as shown in Fig. 5. In the mean time, its propagation velocity increases significantly.

To calculate the propagation velocities of the plasma bullets, the locations of the plasma bullets are determined by the head of the plasma bullets. The details on the propagation velocities of the plasma bullets for different added gases are plotted in Fig. 6. With 1% of N_2 , O_2 , or air flowing from the vertical tube, the plasma bullet propagation velocities increase as soon as the bullets pass through the junction point. On the other hand, the propagation velocity for the case of He only decreases monotonously with distance. It is worth pointing out that propagation behavior for the case of 1% O_2 is quite similar to the case of 1% air.

D. Effects of premixed He/ N_2 , He/ O_2 , and He/air gases

The results shown above confirmed that 1% of N_2 , O_2 , and air added from the vertical tube results in the acceleration

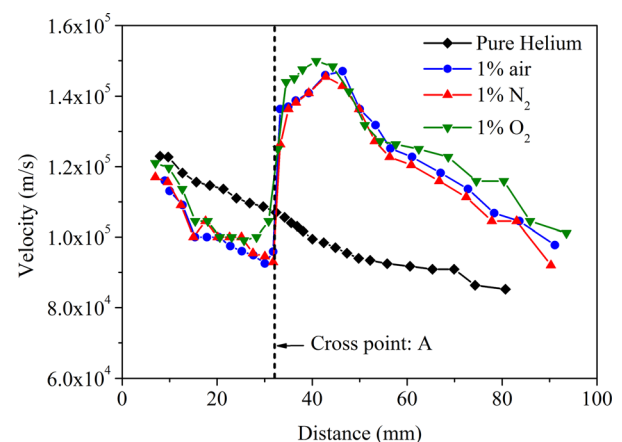


FIG. 6. The propagation velocities *versus* distance along the jet axis for different added gases. All other parameters are the same as in Fig. 2.

of the plasma bullets. Thus, we can conclude that air diffusion plays an important role in the acceleration of the plasma bullets when they exit the nozzle. In the following, to see how the added gases affect the dynamics of the plasma bullets, 1% of N_2 , O_2 , or air are premixed with the main working gas He. Then, the premixed gas is injected into the horizontal tube from the left end.

Figure 7 shows the propagation velocities for the case of He, He/air(1%), He/ N_2 (1%), and He/ O_2 (1%). It is found that the propagation velocities for the case of the three premixed gases are almost the same, which are all higher than the case of He only. It also clearly shows that the velocities for all the premixed gases drop monotonously while they are propagating, which are different from the cases of simulated air diffusion.

E. Effect of permittivity of the dielectric material

To simulate the changes of the permittivity drop when the plasma plumes exit the nozzle, high permittivity materials (glycerol and methyl silicone oil materials) are stuck to the left part of the horizontal tube as shown in Fig. 8. In this way, when the plasma plume propagates from the left (outside with additional material) to the right (outside without additional material), it is similar to the plasma plume propagation from a tube with a high permittivity to a tube with a low permittivity. This propagation is similar to the plasma plume exiting from the nozzle. One advantage of this method is that it does not change the surface characteristics which could also affect the plasma bullet behavior.

Figure 8 shows the propagation velocities of the plasma bullets *versus* distance along the jet axis. The bullet velocities are determined by photographs captured by an ICCD camera. On the left side, when there is a surrounding material, the plasma bullet velocity decreases much more than the case without any additional material on the outside of the tube. The higher the permittivity of the outside material, the faster the propagation velocity decreases. When the plasma bullet propagates from the side with an additional material on the outside of the tube to the side without any addition material on the outside of the tube, the propagation velocities

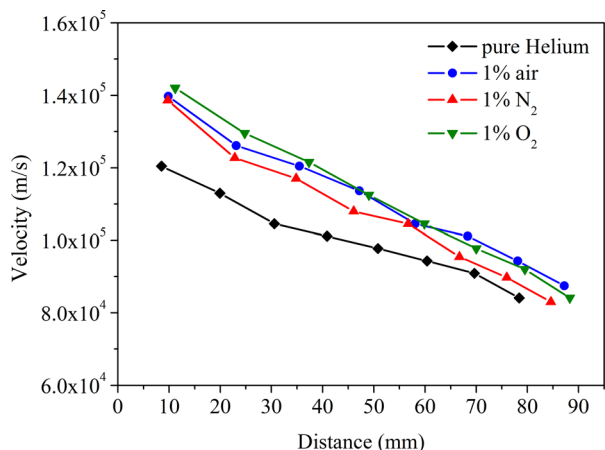


FIG. 7. The propagation velocities *versus* distance along the jet axis for different premixed gases from the horizontal tube. All other parameters are the same as that in Fig. 2.

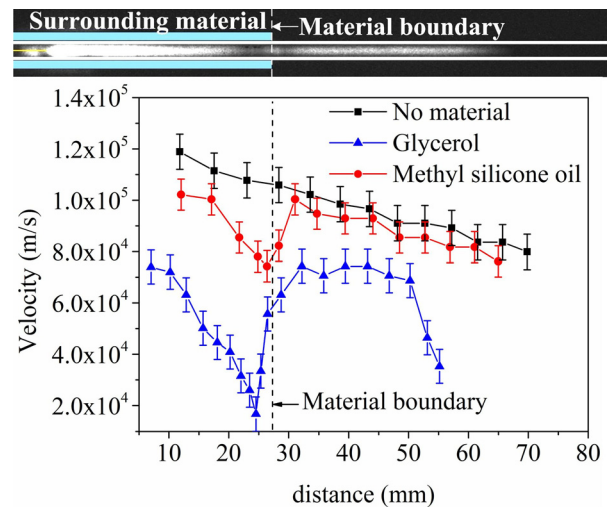


FIG. 8. The propagation velocities *versus* distance along the jet axis for the cases of (1) tube only, (2) glycerol, and (3) methyl silicone oil sticking to the outside of the left part of the tube. The dielectric constants for glycerol and methyl silicone oil materials are 47 and 2.8, respectively. The surrounding materials also have tube shape. The thickness of the surrounding materials is the same of 2 mm. He flow rate: 1 l/min. The electric parameters are the same as in Fig. 2.

of the bullets increase dramatically. This result tells us that the acceleration behavior of the plasma plumes when they exit a nozzle is also related to the permittivity change.

F. Effects of added gases on electric field strength

Because the plasma plume propagation is driven by the electric field, to find out whether the electric field strength increases around the cross point of the T shape tube when 1% of N_2 , O_2 , or air is added, we measured the electric field strength in the plasma bullet by fitting the π -polarized spectra of He 447 nm line. This method is based on the application of the polarization-dependent Stark splitting and shifting of He 447 nm line and its forbidden counterpart. Details about the method can be found in Refs. 31–34. With the polarizer mounted with the axis of the plasma jet parallel to the external electric field, three components can be detected: allowed line ($2p^3P^0-4d^3D^0$), forbidden counterpart ($2p^3P^0-4f^3F^0$), and a E-free component. Separation between the peaks of the allowed line and the forbidden line depends on the electric field strength.^{33,34} In this experiment, optical emission from the plasma plume is polarized in the axial electric field direction by using a plastic polarizer and detected by an ICCD camera. The ICCD camera is triggered with a time delayed pulse, synchronized with the applied pulse voltage. The gate duration of the ICCD was 20 ns. The entrance slit of the spectrometer is 30 μ m and the grating of the spectrometer is 3600 grooves per mm. The instrumental pseudo-Voigt profile width is 0.05 nm.

Figure 9(a) shows that the electric field strength for the case of He only remains almost unchanged at 15.5 kV/cm for the distance up to about 42 mm. On the other hand, with 1% of added O_2 from the vertical tube, the electric field strength decreases as it approaches to the junction point of T shape tube, and it increases from 15 kV/cm to 16.5 kV/cm as it passes through the junction point. This result is consistent with the

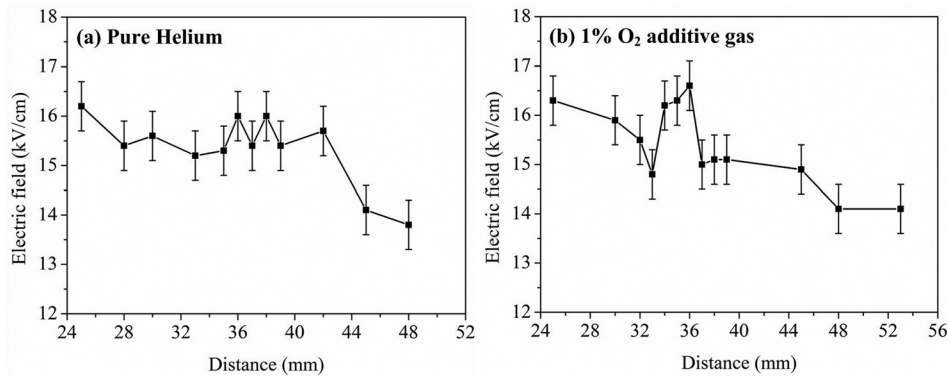


FIG. 9. The spatial distribution of electric field strength along the jet axis for (a) pure He and (b) 1% O_2 added gas. The other parameters are the same as in Fig. 2.

results of the propagation velocities shown in Fig. 6. In addition, the measured value of the electric field is also in fairly good agreement with the model predictions.^{16–19} The results for 1% of N_2 and air are similar with 1% of O_2 .

IV. DISCUSSION AND CONCLUSION

When 1% of the N_2 , O_2 , or air is added to the main working gas from the vertical tube, the plasma bullets accelerate. This is due to the low ionization energy of N_2 and O_2 molecules and the Penning reactions between the He metastable states and N_2 and O_2 molecules, which enhance the volume ionization and accelerate the propagation of the plasma bullet.^{27,35,36} These results are consistent with the results when premixed added gases are used. Thus, it is concluded that air diffusion and Penning ionization play an important role in the acceleration behavior of the plasma bullets when they exit the nozzle.

Besides, when the plasma plumes propagate from a tube with the high permittivity to the low permittivity region, the propagation velocities also increase. The higher the difference of the permittivity of the materials surrounding the plasma, the more the propagation velocities increase. Therefore, it can be also concluded that the permittivity change of the medium surrounding the plasma plumes when they exit the nozzle also play an important role in the acceleration behavior. While the plasma bullet accelerates, the electric field of the plasma bullet increases, which confirms that the plasma plume propagation is electric field driven.

It is worth emphasizing that, when 1% of N_2 or O_2 is added, the propagation velocities for both cases increase. But there is no difference between the cases of N_2 and O_2 . This is surprising and the mechanism on this observation requires further investigation.

ACKNOWLEDGMENTS

This work was partially supported by the National Natural Science Foundation (Grant Nos. 51077063 and 51277087), Research Fund for the Doctoral Program of Higher Education of China (No. 20100142110005), and Chang Jiang Scholars Program, Ministry of Education, People's Republic of China.

¹K. Ostrikov, E. C. Neyts, and M. Meyyappan, *Adv. Phys.* **62**, 113 (2013).

²M. Keidar and I. Beilis, *J. Appl. Phys.* **106**, 103304 (2009).

³S. Reuter, K. Niemi, V. Gathern, and H. Dobeles, *Plasma Sources Sci. Technol.* **18**, 015006 (2009).

⁴A. Shashurin, M. Keidar, S. Bronnikov, R. A. Jurjus, and M. A. Stepp, *Appl. Phys. Lett.* **93**, 181501 (2008).

⁵D. B. Graves, *J. Phys. D: Appl. Phys.* **45**, 263001 (2012).

⁶G. Fridman, A. Brooks, M. Galasubramanian, A. Fridman, A. Gutsol, V. Vasilets, H. Ayan, and G. Friedman, *Plasma Processes Polym.* **4**, 370 (2007).

⁷M. Laroussi, *IEEE Trans. Plasma Sci.* **37**, 714–725 (2009).

⁸X. Zhang, D. Liu, R. Zhou, Y. Song, Y. Sun, Q. Zhang, J. Niu, H. Fan, and S. Yang, *Appl. Phys. Lett.* **104**, 043702 (2014).

⁹X. Lu, T. Ye, Y. Cao, Z. Sun, Q. Xiong, Z. Tang, Z. Xiong, J. Hu, Z. Jiang, and Y. Pan, *J. Appl. Phys.* **104**, 053309 (2008).

¹⁰X. Lu, Z. Jiang, Q. Xiong, Z. Tang, X. Hu, and Y. Pan, *Appl. Phys. Lett.* **92**, 081502 (2008).

¹¹X. Lu, M. Laroussi, and V. Puech, *Plasma Sources Sci. Technol.* **21**, 034005 (2012).

¹²X. Lu and M. Laroussi, *J. Appl. Phys.* **100**, 063302 (2006).

¹³B. Sands, B. Ganguly, and K. Tachibana, *Appl. Phys. Lett.* **92**, 151503 (2008).

¹⁴X. Lu, G. V. Naidis, M. Laroussi, and K. Ostrikov, *Phys. Rep.* **540**, 123(2014).

¹⁵X. Zhang, D. Liu, Y. Song, Y. Sun, and S. Yang, *Phys. Plasmas* **20**, 053501 (2013).

¹⁶G. Naidis, *J. Phys. D: Appl. Phys.* **43**, 402001 (2010).

¹⁷G. Naidis, *J. Phys. D: Appl. Phys.* **44**, 215203 (2011).

¹⁸D. Breden, K. Miki, and L. Raja, *Plasma Sources Sci. Technol.* **21**, 034011 (2012).

¹⁹D. Breden, K. Miki, and L. Raja, *Appl. Phys. Lett.* **99**, 111501 (2011).

²⁰J. Boeuf, L. Yang, and L. Pitchford, *J. Phys. D: Appl. Phys.* **46**, 015201 (2013).

²¹Z. Xiong, E. Robert, V. Sarron, J. Pouvesle, and M. Kushner, *J. Phys. D: Appl. Phys.* **45**, 275201 (2012).

²²Z. Xiong and M. Kushner, *Plasma Sources Sci. Technol.* **21**, 034001 (2012).

²³Q. Xiong, X. Lu, Y. Xian, J. Liu, C. Zou, Z. Xiong, W. Gong, K. Chen, X. Pei, F. Zou, J. Hu, Z. Jiang, and Y. Pan, *J. Appl. Phys.* **107**, 073302 (2010).

²⁴N. Mericam-Bourdet, M. Laroussi, A. Begum, and E. Karakas, *J. Phys. D: Appl. Phys.* **42**, 055207 (2009).

²⁵E. Karakas and M. Laroussi, *J. Appl. Phys.* **108**, 063305 (2010).

²⁶S. Wu, Q. Huang, Z. Wang, and X. Lu, *IEEE Trans Plasma Sci.* **39**, 2286 (2011).

²⁷F. Liu, D. Zhang, and D. Wang, *Thin Solid Films* **521**, 261–264 (2012).

²⁸J. Jansky and A. Bourdon, *Appl. Phys. Lett.* **99**, 161504 (2011).

²⁹See <http://www.fluent.com> for Computational Fluid Dynamics (CFD).

³⁰S. Wu, Q. Huang, Z. Wang, and X. Lu, *J. Appl. Phys.* **113**, 043305 (2013).

³¹G. Sretenovi, I. Krsti, V. Kovaevi, B. Obradovic, and M. Kuraica, *Appl. Phys. Lett.* **99**, 161502 (2011).

³²B. Obradovic and M. Kuraica, *Phys. Lett. A* **372**, 137–140 (2008).

³³M. Kuraica and N. Konjevic, *Appl. Phys. Lett.* **70**, 1521–1523 (1997).

³⁴B. Obradović, S. Ivković, and M. Kuraica, *Appl. Phys. Lett.* **92**, 191501 (2008).

³⁵Y. Sakiyama, D. B. Graves, J. Jarrige, and M. Laroussi, *Appl. Phys. Lett.* **96**, 041501 (2010).

³⁶Q. Li, W. Zhu, X. Zhu, and Y. Pu, *J. Phys. D: Appl. Phys.* **43**, 382001 (2010).